UCRL-JC-124895
PREPRINT

Spatial Filter Issues

J. E. Murray, K. G. Estabrook, D. Milam,
W. D. Sell, B. M. Van Wonterghem,
M. D. Feit, and A. M. Rubenchik

This paper was prepared for submittal to the
2nd Annual International Conference on Solid-State
Lasers for Application to Inertial Confinement Fusion
Paris, France
October 22-25, 1996

December 9, 1996

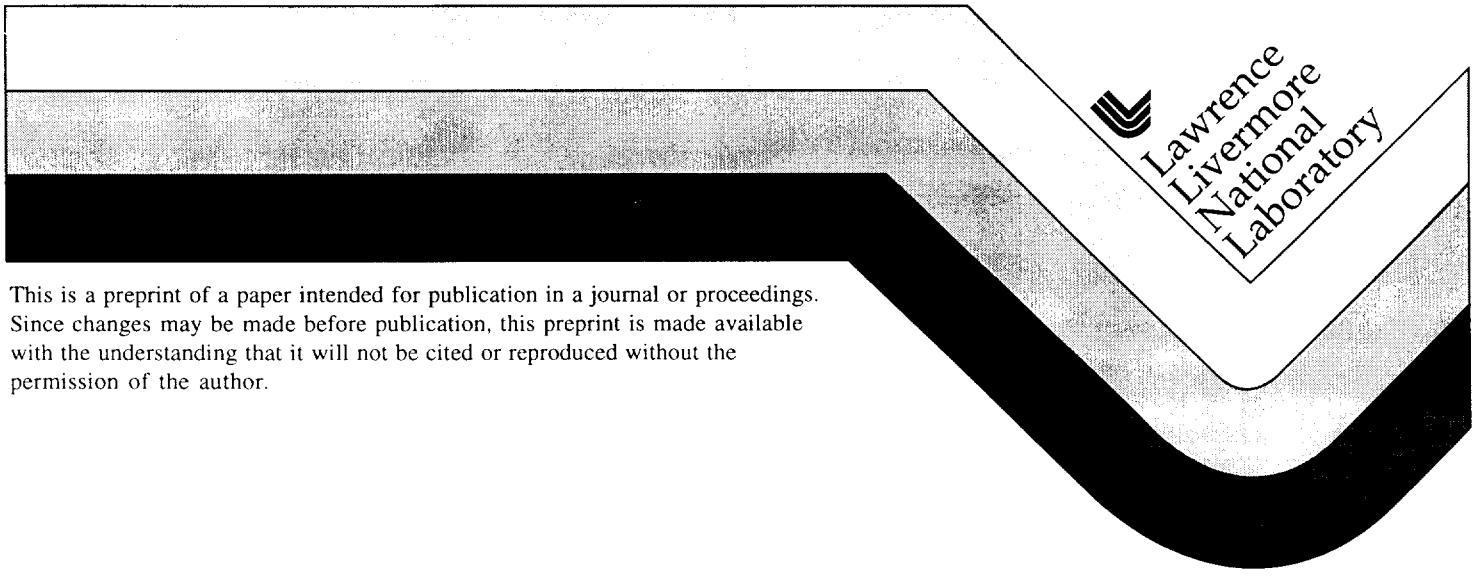

Spatial filter issues*

James E. Murray, Kent G. Estabrook, David Milam, Walter D. Sell, Bruno M. Van Wonterghem, Mike D. Feit, Alexander M. Rubenchik

Lawrence Livermore National Laboratory
P. O. Box 808, Livermore, CA 94550

ABSTRACT

Experiments and calculations indicate that the threshold pressure in spatial filters for distortion of a transmitted pulse scales approximately as $I^{-0.2}$ and $(F\#)^2$ over the intensity range from 10^{14} to $2x10^{15}$ W/cm^2. We also demonstrated an interferometric diagnostic that will be used to measure the scaling relationships governing pinhole closure in spatial filters. Key words: laser, spatial filter pressure, pinhole closure, optical gas breakdown,

1. INTRODUCTION

Large vacuum spatial filters are essential for high energy fusion laser systems. They relay image the beam profile over large distances and strip undesirable spatial noise from the beam, thereby maintaining beam quality on the optics. The 192 beam National Ignition Facility (NIF) uses two spatial filters per beamline, a 22-meter long spatial filter in a four-pass amplifier cavity and a 60-meter long spatial filter to transport the output beam to the target chamber.

The size and performance requirements of NIF require a careful analysis of four interrelated issues regarding spatial filters: maximum background pressure, pinhole closure, beam dumps, and ablation contamination from pinholes and beam dumps. This paper deals with pressure and pinhole closure. The remaining two issues are addressed in this same session in "Development of long-lifetime, low-contamination beam dumps for NIF" by Mary A. Norton, et al.

2. MAXIMUM PRESSURE

Design engineers for the NIF Project need to know at what pressure to operate spatial filters. Operating at higher pressure reduces cost, because it reduces the size of the vacuum pump required. It also potentially reduces contamination on optical surfaces from pinholes and beam dumps by reducing the mean-free-path of ablation products. However, too high a pressure results in distortion of the transmitted pulse, due to refraction or absorption in the ionized background gas in the focal region of the spatial filter. We define a threshold pressure p(th) as that pressure at which distortion of the transmitted pulse first appears, and we recommend a maximum operating pressure of about p(th)/10. We have investigated p(th) both theoretically and experimentally for the NIF transport and cavity spatial filters.

We plan to use tests on the NIF beamline prototype, called Beamlet, to confirm our modeling of p(th). p(th) potentially depends on F# (ratio of lens focal length to beam diameter at the lens) as well as the power and temporal length of the pulse into the spatial filter. However, the NIF transport spatial filter (TSF) has a different F# than the Beamlet spatial filters, so Beamlet cannot simultaneously test at the same F# and power. The F#s of the NIF TSF and cavity spatial filter (CSF) are 81 and 32, respectively. The worst-case pulse for gas breakdown will be the highest power pulse, about 5.5 TW at the NIF TSF and 2.2 TW at the NIF CSF. The Beamlet spatial filters are both F/28, which allows a good test for the NIF CSF, but requires reducing the beam size to reach the F/81 of the NIF TSF. At the reduced beam size (about 3x smaller), the maximum output of Beamlet will be about 10x lower than the 5.5 TW expected in the NIF TSF. Consequently, we need a model for the scaling of p(th) with F# and power, as well as these Beamlet tests.

We have done a series of calculations and experiments to establish the scaling laws for p(th). The experiments were done on an off-line laser facility called the Optical Sciences Laboratory (OSL), and the calculations were done with LASNEX[1]. Figure 1 shows experimental data and calculations for p(th) plotted versus intensity at focus for three different F#s. The points indicate experimental data taken with the 1053 nm, ~1.2x diffraction-limited OSL laser. The test chamber was evacuated to less than 10^{-4} Torr and back-filled with ambient air to the desired pressure. We found that the near-field distribution of the transmitted pulse was the most sensitive indicator of p(th), and that p > p(th) caused low-spatial-frequency distortion. We defined p(th) as that pressure output of the OSL. Solid vertical lines in the figure connect calculations which gave above and below threshold

* This work was performed under the auspices of the U.S. Department of Energy by the Lawrence Livermore National Laboratory under contract No. W-7405-Eng-48.

which first altered the near-field distribution. The experimental data is limited in intensity by the maximum safe

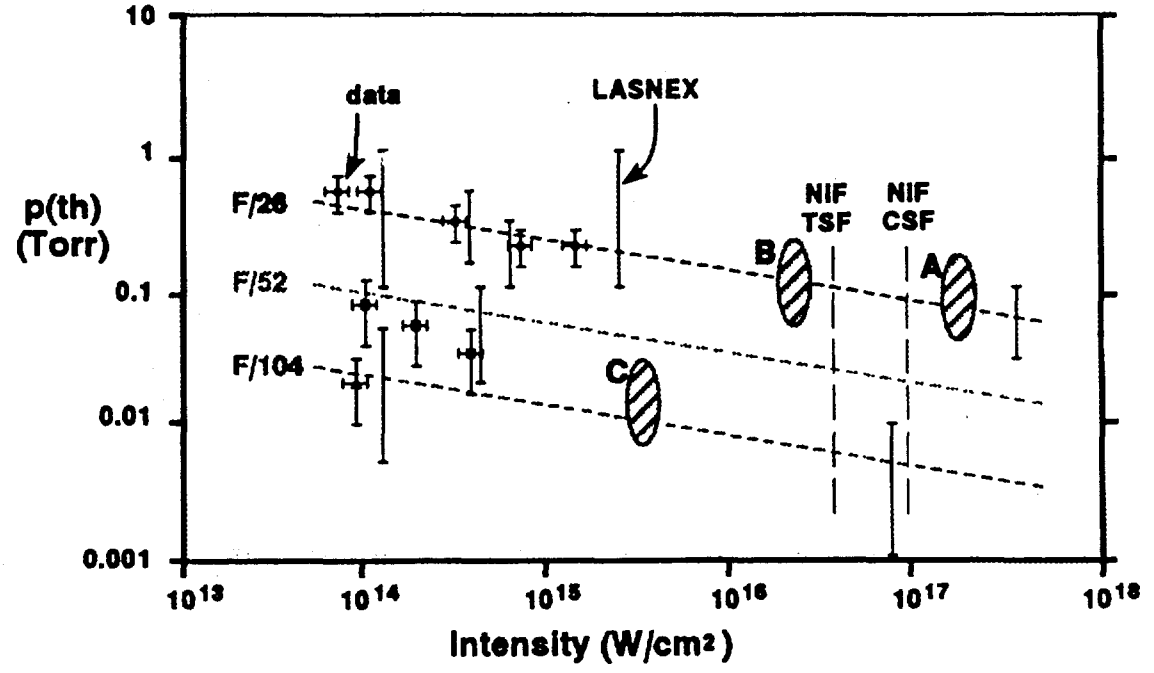

Figure 1 Experimental data and calculations for threshold pressure.

results. The two vertical dashed lines indicate the worst-case intensities expected for the NIF TSF and CSF. The figure shows that our calculations agree well with the experimental data.

The upper dashed line in Fig. 1 is an approximate fit to the F/26 data and calculations, and it shows p(th) decreasing with intensity (I) as $p(th) \sim I^{-0.2}$. Calculations show that at intensities greater than about 10^{14} W/cm^2, all the atoms are at least singly ionized. Therefore, increasing intensity liberates more electrons per atom and consequently reduces p(th), but only slowly, because of the increased binding energy of each successive electron. We would expect p(th) to vary inversely as the interaction length, because the angular deflection of a ray depends directly on the length over which it interacts with an electron density gradient as well as the magnitude of the gradient. Consequently, we expect $p(th) \sim (F\#)^{-2}$, since the length of the focal region increases as $(F\#)^2$. The dashed lines at F/52 and F/104 are scaled from the F/26 line assuming $p(th) \sim (F\#)^{-2}$, and they are at least consistent with both data and calculations.

The p(th) observations on the OSL did not indicate a dependence on pulse length. For shots between 50 and 100 TW/cm^2, pulse lengths of 1, 5, and 20 ns gave p(th) values of 0.4 ± 0.15, 0.6 ± 0.1, and 0.5 ± 0.15 Torr, respectively, essentially the same within experimental error. Similarly, for shots between 250 and 300 TW/cm^2, pulse lengths of 1 and 5 ns gave p(th) values of 0.2 ± 0.1 and 0.4 ± 0.1 Torr, respectively, which are also not significantly different given the experimental error. A practical consequence is that the gas breakdown tests on Beamlet can be conducted with short pulses (~1 ns) to reduce the threat of damage to Beamlet components.

We plan to confirm the above scaling of p(th) with intensity and F# at near-NIF intensities by taking additional data on Beamlet in the regions A, B, and C in Fig. 1. At F/28 we will confirm p(th) at an intensity higher than expected in the NIF CSF with a measurement at A, and confirm scaling with intensity with a measurement at B. At F/81, we will confirm F# scaling with a measurement at C. If these values fall in the expected range, we will be confident to predict p(th) for the NIF TSF.

If the above scaling holds, the p(th) values for the NIF CSF and TSF will be 0.1 Torr and .005 Torr, respectively. These would mean recommended maximum operating pressures of about .01 Torr and .0005 Torr. NIF is currently designed to operate both filters at .0001 Torr, so there would be little room to increase the TSF specification, but the CSF specification could be increased significantly.

3. PINHOLE CLOSURE

Pinhole closure is an issue for NIF, because the required 21-ns pulselengths are much longer than used on previous lasers. Also, we would like to run smaller pinholes on NIF than used previously, ±130 μrad in the CSF and ±100 μrad in the TSF. Figure 2 shows a schematic of

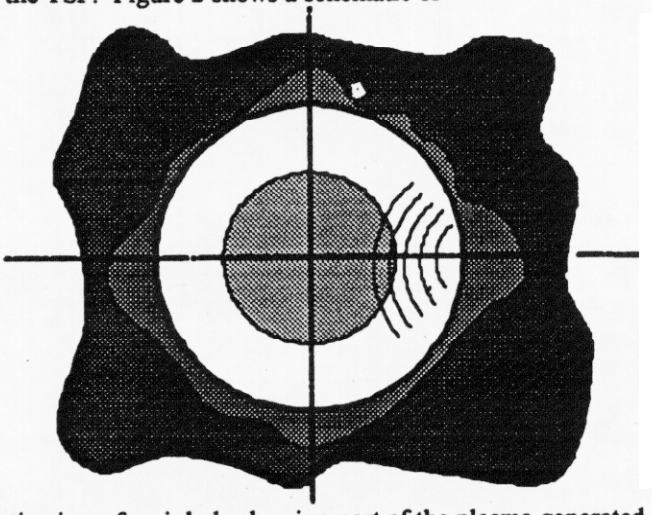

Figure 2. Schematic view of a pinhole showing part of the plasma generated at the edge, propagating into the main part of the pulse.

the pinhole region, looking at the pinhole along the direction of the incoming laser. The desired pinholes are 3.1 mm in diameter for the CSF and 6.1 mm for the TSF. The shaded region in the center of the figure corresponds to the portion of the far field that must pass through the pinhole to avoid introducing unacceptable modulation on the near field of the transmitted pulse. For a beam with a square, 92% fill factor near field, this region occupies more than 50% of the diameter of a ±100 μrad pinhole along the directions of the sides of the square beam profile.

The lightly shaded region outside the edge of the pinhole in Fig. 2 indicates the portion of the far field blocked by the pinhole. Estimates of the intensities in this region range from 10^{11}- 10^{13} W/cm^2 and are based on Schlieren measurements from Beamlet and propagation calculations assuming the transmitted wave-front requirements for NIF optics. At these intensities, any pinhole material will generate a plasma, which expands into the pinhole. If this plasma reaches the central region with enough density to refract or absorb significantly, it will introduce spatial modulation on the transmitted beam. Previously reported velocities to completely close pinholes[2,3] range from 0.1 to 0.5 mm/ns. This means that even at the slowest of these velocities, a plasma of significant density will reach the central region of either of the NIF pinholes during a 21-ns pulse.

Recent measurements[5] show that refraction occurs substantially before complete pinhole closure. As a result, we define "closure" in terms of a change to the transmitted near-field beam profile, and we anticipate faster closure velocities for this definition than those previously reported for complete closure.

Experience with various types of pinholes shows that pinhole geometry can influence closure times. The left side of Fig. 3a shows a standard washer-type pinhole
from the direction of the incoming beam, and the right side shows a longitudinal cross section. The longitudinal extent of the pinhole is typically small compared to its diameter. Most of the previous measurements were made on washer-type pinholes[2,3,4]. Closure velocities for this pinhole are too large for NIF pulse lengths.

A second type of pinhole which is currently in use in the Nova output spatial filters is shown in Fig. 3b. This pinhole is divided azimuthally into four segments, which are offset from one another longitudinally. The effect is to reduce the radial convergence of the plasma and prevent stagnation of the plasma on axis. Nova operators report that these pinholes stay open longer than corresponding washer-type pinholes. This result alone demonstrates that pinhole geometry can increase the time to pinhole closure.

Figure 3c shows our most promising pinhole geometry[5]. It consists of a large aspect ratio cone, with a length as much as 30 times its diameter, and with the defining aperture at the output end of the cone. The input diameter is typically about twice the output diameter. This geometry increases closure time by increasing the diameter of the entrance hole, which places the entrance aperture in a lower intensity portion of the beam and increases the area over which the power is distributed. It also reduces plasma formation at the interior surface by

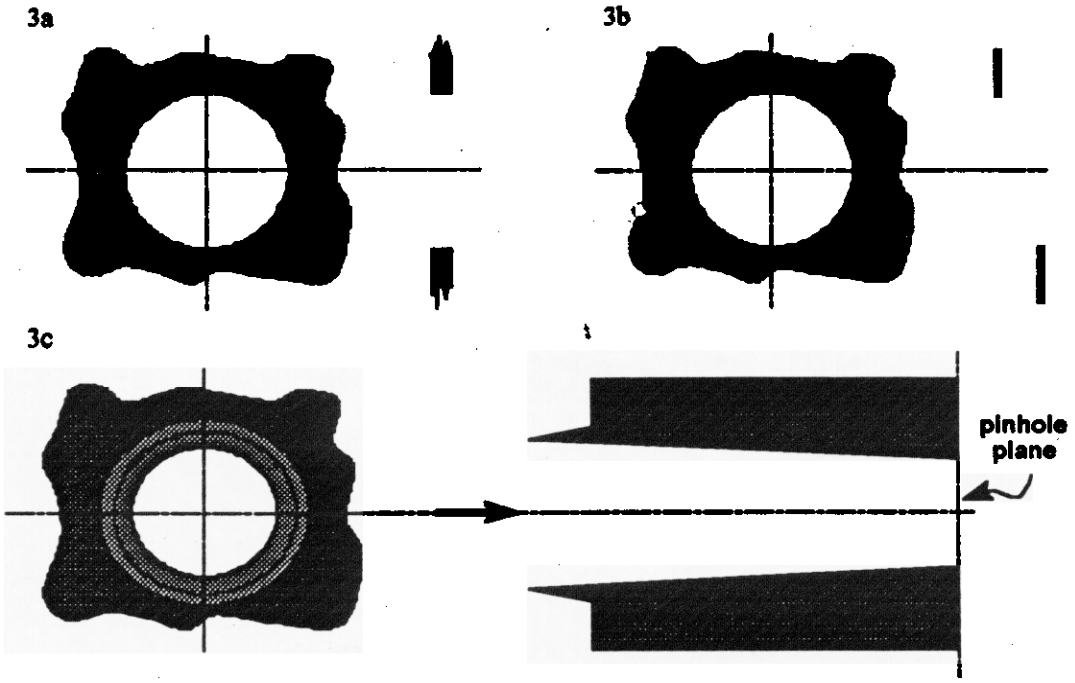

Fig. 3 Schematics of 3 pinhole types: the standard washer-pinhole; a thin, azimuthally segmented pinhole; and a conical pinhole.

reflecting or refracting rather than absorbing incoming laser energy. LASNEX calculations predict that conical pinholes will stay open two to three times longer than comparable washer-type pinholes, and initial measurements[5] agree. Streaked near-field data showed that a conical pinhole with a 900-μm entrance hole and a 500-μm exit hole stayed open about two times longer than 500-μm diameter washer pinhole.

Although the conical pinhole clearly remains open longer than a washer-type pinhole, its geometry has not yet been optimized, and other geometries might perform even better. However, further progress requires a better understanding of pinhole closure physics. We need to know how closure time scales with laser pulse parameters, like intensity, fluence, and pulse shape, as well as with pinhole material and angle of incidence. We also need to be able to relate closure times to measurable and calculable quantities like electron density gradients and interaction lengths. We plan to measure scaling laws using the OSL and to relate closure to calculable quantities using Beamlet. We will also test any new pinhole geometries on Beamlet.

For both OSL and Beamlet experiments, we will use a probe beam and streaked interferometer to diagnose pinhole closure, as shown in Fig. 4. One arm of a Mach-Zender interferometer will pass through the pinhole during the time of the main pulse. Phase differences from transmission through the plasma in the pinhole cause

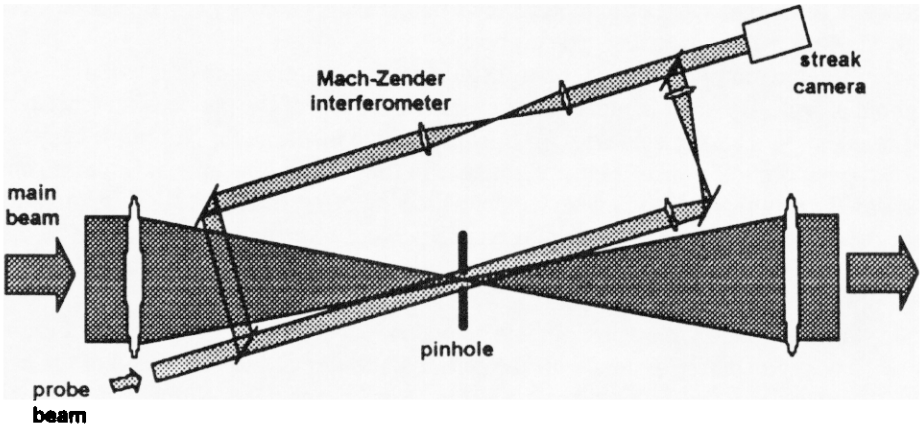

Fig. 4 Schematic of pinhole closure diagnostic.

changes to the interference pattern. A streak camera or framing camera will give time resolution.

Initial measurements on the OSL show the value of this diagnostic for determining scaling laws. Figure 5 shows a streaked interferogram of a stainless steel knife-edge irradiated at $2x10^{12}$ W/cm^2. Time increases to the right, with zero indicating the start of the 5-ns square main pulse. The full-width-half-maximum size of the

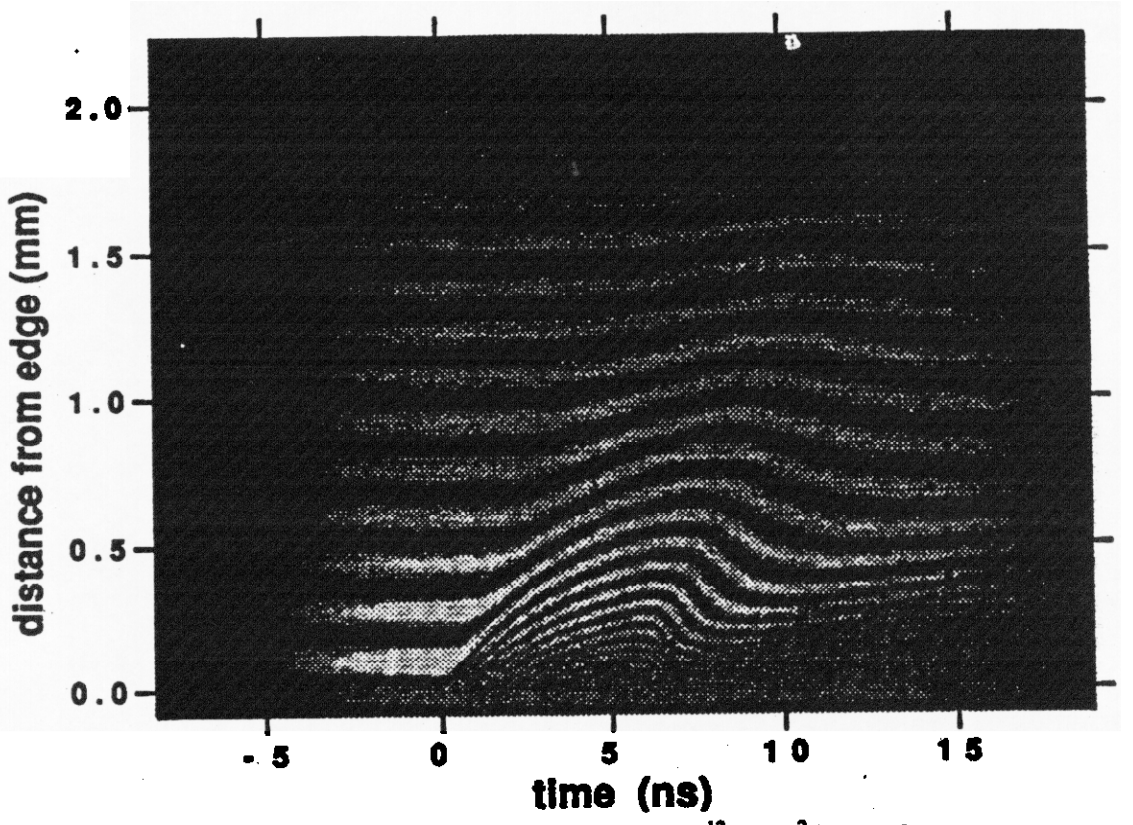

Fig. 5 Streaked interferogram of a knife-edge irradiated by a 5-ns $2x10^{12}$ W/cm^2 laser pulse.

main beam at the knife edge was about 0.3 mm with about half hitting the knife-edge. The vertical axis in the figure shows distance from the initial position of the knife-edge in millimeters. From this data, the first half-wave of phase perturbation moves away from the knife-edge with an initial velocity of 0.2 mm/ns. Changing pulse parameters, knife-edge materials, and angles of incidence of the main pulse on the knife-edge will provide a direct comparison of these changes.

4. SUMMARY

Off-line measurements and calculations indicate that the threshold pressure in spatial filters scales as $I^{-0.2}$ and $(F\#)^{-2}$, between 10^{14} and $2x10^{15}$ W/cm^2. Extrapolating to NIF conditions gives predicted values of 0.1 Torr for the CSF and .005 Torr for the TSF. We are planning to test these predictions on Beamlet at closer-to-NIF intensities. Regarding pinhole closure, we demonstrated an interferometric diagnostic that will be used to measure the scaling relationships governing pinhole closure.

5. REFERENCES

1.) G. B. Zimmerman, W. L. Kruer, Comments in Plasma Physics & Controlled Fusion 2, p51, 1977.

2.) J. S. Pearlman, J. P. Anthes, "Closure of pinholes under intense laser radiation", Applied Optics 16, 8, 8/77, 2328 - 31.

3.) J. M. Auerbach, N. C. Holmes, J. T. Hunt, G. J. Linford, "Closure phenomena in pinholes irradiated by Nd laser pulses", Applied Optics 18, 14, 7/15/79, 2495 - 99.

4.) S. A. Dimakov, S. I. Zavgorodneva, L. V. Koval'chuk, A. Yu. Rodionov, "Investigation of the threshold of formation of a plasma screening radiation in a spatial filter", Sov. J. Quantum Electron. 19, 6, 6/89, 803-5.
5.) P. Celliers, K. Estabrook, R. J. Wallace, J. E. Murray, L. B. Da Silva,
B. J. MacGowan, B. M. Van Wonterghem, J. T. Hunt, K. Manes, "A novel spatial filter pinhole for high energy pulsed lasers", 24th European Conference on Laser Interaction with Matter, University of Madrid, Madrid, Spain, 3-7 June 1996